Resonantly Enhanced Multiphoton Ionization and Zero Kinetic Energy Photoelectron Spectroscopy of Chrysene: A Comparison with Tetracene

ARTICLE *in* THE JOURNAL OF PHYSICAL CHEMISTRY A · MAY 2012

Impact Factor: 2.69 · DOI: 10.1021/jp303323e · Source: PubMed

3 AUTHORS, INCLUDING:

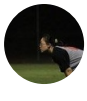

Jie Zhang
Oregon State University
18 PUBLICATIONS **130** CITATIONS

SEE PROFILE

THE JOURNAL OF PHYSICAL CHEMISTRY A

Article

pubs.acs.org/JPCA

Resonantly Enhanced Multiphoton Ionization and Zero Kinetic Energy Photoelectron Spectroscopy of Chrysene: A Comparison with Tetracene

Jie Zhang, Colin Harthcock, and Wei Kong*

Department of Chemistry, Oregon State University, Corvallis, Oregon 97331-4003, United States

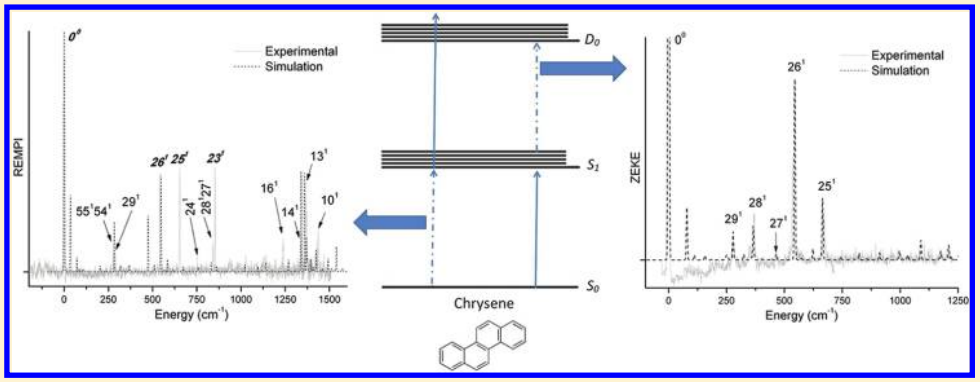

ABSTRACT: We report the electronic and vibrational spectroscopy of chrysene using resonantly enhanced multiphoton ionization (REMPI) and zero kinetic energy (ZEKE) photoelectron spectroscopy. As an isomer of tetracene, chrysene contains a kink in the middle of the four fused hexagonal rings, which complicates not just the symmetry but, more importantly, the molecular orbitals and hence vibronic transitions. Incidentally, the two nearby electronically excited states of chrysene have the same symmetry, and vibronic coupling introduces no out-of-plane vibrational modes. As a result, the REMPI spectrum of chrysene contains essentially only in-plane ring deformation modes, similar to that of tetracene. However, density functional calculations using Gaussian even after the inclusion of vibronic coupling can only duplicate the observed REMPI spectrum in a qualitative sense, and the agreement is considerably worse than our recent work on a few pericondensed polycyclic aromatic hydrocarbons and on tetracene. The ZEKE spectrum of chrysene via the origin band of the intermediate electronic state S_1, however, can be qualitatively reproduced by a straightforward Franck−Condon calculation. The ZEKE spectra from vibrationally excited states of the S_1, on the other hand, demonstrate some degree of mode selectivity: the overall intensity of the ZEKE spectrum can vary by an order of magnitude depending on the vibrational mode of the intermediate state. A scaling factor in the theoretical vibrational frequency for the cation is also needed to compare with the experimental result, unlike tetracene and pentacene.

INTRODUCTION

Polycyclic aromatic hydrocarbons (PAHs) are a class of compounds consisting of more than two fused aromatic rings without any heteroatoms or substituents. Depending on the number of shared carbon atoms between adjacent hexagonal rings, PAHs can be further separated into two categories: cata-condensed species with no carbon atoms shared by more than two rings and, otherwise, peri-condensed species. Although conceptually simple in atomic structure, PAHs have a range of properties in electronic structures.[1−3] As a few groups including our own have discovered, many PAHs exhibit strong configuration interactions, and great care has to be exerted in calculating properties of excited electronic states.[4−10] Closely spaced electronic states complicate the assignment of vibronic transitions, and vibronic coupling in PAHs is prevalent.[11] The chemical stability and structural rigidity of these species are tied to the detailed connectivity of each carbon atom and the symmetry of the overall molecular structure.

Aside from their fundamental interest in physical chemistry, PAHs are also studied in environmental sciences because of incomplete combustion of carbonaceous fuels,[12,13] in biology because of their carcinogenicity,[14−17] in molecular electronics because of their readily available mobile π electrons,[18−20] and in astrophysics as a candidate species in the interstellar medium.[21−29] The possibility of neutral and charged PAHs as carriers of the unidentified infrared bands and/or diffuse interstellar bands has been investigated for over four decades. Apart from identification of functional groups in the mid-infrared (MIR) spectral region, however, confirmation of specific PAHs in the interstellar medium is still yet to be achieved.[25,30−32] Establishment of a database in the fingerprint far-infrared (FIR) region of PAHs and their cationic and

Received: April 6, 2012
Revised: May 24, 2012
Published: May 30, 2012

anionic species is therefore instrumental for the next phase of space exploration.

Our research group has been engaged in a series of investigations of PAH cations in the far-infrared using resonantly enhanced multiphoton ionization (REMPI) and zero kinetic energy (ZEKE) photoelectron spectroscopy.[8−10,33,34] We have reported spectroscopic analysis of cata-condensed species including tetracene and pentacene and peri-condensed species including pyrene, benzo[*a*]pyrene (B*a*P), and benzo[*g*,*h*,*i*]perylene (B*ghi*P). In this work, we report another cata-condensed species, chrysene, an isomer of tetracene but with a kink in the chain of the fused hexagonal rings. We analyze the observed vibronic transitions of the excited electronic state based on density functional theory (DFT) calculations using the Gaussian 09 suites,[35] but with a cautious interpretation of the theoretical result. We notice that the kink in the chain structure has a profound effect on the molecular orbitals of chrysene. Furthermore, the stability of ZEKE Rydberg states demonstrates mode dependence, implying a mode-specific decay mechanism of the relevant states. This situation is drastically different from the other two cata-condensed species tetracene and pentacene.[33,34] Rather, the complication of the molecular orbitals is similar to that of a peri-condensed species, pyrene.[8] Our results on chrysene will be compared with previous reports using several different experimental techniques.[3,36−39] In addition, we offer the first experimental result on several a_g modes of this C_{2h} molecular cation in the FIR. Assignment of these bands further provides a scaling factor of 0.9766, which is smaller than those from our previous studies of PAHs and quite different from those of tetracene and pentacene. Our results, in combination with those from matrix isolation studies, offer the possibility of fitting both IR-active and -forbidden modes of chrysene cation from FIR to MIR.[40,41]

EXPERIMENTAL SECTION

The experimental apparatus and procedure have been published earlier.[8,33] The title compound chrysene (Aldrich) was heated to 200 °C for sufficient vapor pressure, and a small time-of-flight mass spectrometer confirmed the intact molecular structure of the sample. In the REMPI experiment, the ionization laser was set at 300 nm while the resonant laser scanned across the vibronic structures of the first excited electronic state of chrysene. In the ZEKE experiment, the resonant laser was set at the chosen vibronic structure from the REMPI experiment while the ionization laser scanned across the ionization threshold. The delay time of the pulsed electric field from the ionization laser was 1−2 μs in a DC spoiling field of ∼1 V/cm, and the amplitude of the electric pulse was ∼5 V/cm.

RESULTS

Two-Color 1 + 1′ REMPI Spectroscopy. The two-color 1 + 1′ REMPI spectrum of chrysene near the origin of the $S_1 \leftarrow S_0$ electronic transition is displayed in Figure 1. The observed lowest energy transition is also the most intense in the spectrum, and it is assigned as the origin band. To emphasize the frequencies of the observed vibronic bands, the spectrum in Figure 1 is shifted by 28 195 cm^{-1}, i.e., the transition energy of the electronic origin. The wavelengths of the lasers have been calibrated using neon transitions from an optogalvanic lamp,

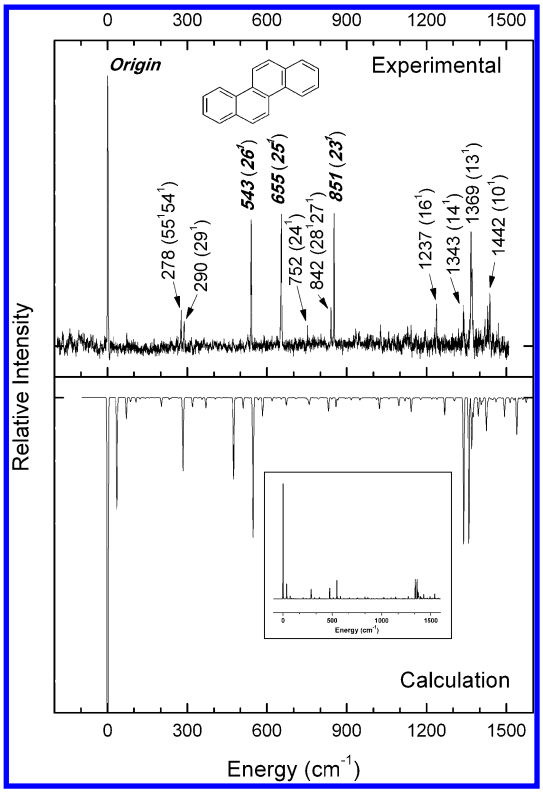

Figure 1. 1 + 1′ REMPI spectrum of jet-cooled chrysene. The spectrum is shifted by 28 195 cm^{-1} (the origin of the electronic transition) to highlight the frequencies of the different vibronic transitions. The molecular structure is also included in the inset. The top panel is the experimental spectrum, and the calculation using the Franck−Condon principle in the bottom panel is inverted for comparison. The inset shows the overall intensity distribution without scaling of the origin band. Only the bold-faced transitions have yielded observable ZEKE spectra, as shown in Figure 2.

and the uncertainty in wavelength is about 1 cm^{-1}. The observed line width, on the other hand, is 3−4 cm^{-1}.

We have performed calculations of both the ground and excited electronic states of chrysene using the Gaussian 09 suite[35] to assist with the spectroscopic assignment. The ground electronic state was obtained from the density functional theory method and the B3LYP functional with the 6-311G(d,p) basis set. For the excited electronic state, time-dependent density functional theory (TDDFT) with the 6-31G(d,p) basis set was used. The REMPI spectrum was calculated with the Herzberg−Teller (HT) vibronic coupling option. The resulting spectrum is also plotted in Figure 1 for comparison.

The calculation is only in qualitative agreement with the experimental results, and the agreement is substantially inferior to our previous work on B*a*P and B*ghi*P.[9,10] Other than the overly strong origin band, the cluster of modes 23−26 misses two major peaks, and modes 13 and 14 are also mismatched in intensity. Nevertheless, this degree of agreement offers some guidance to the assignment of the observed vibronic bands. Table 1 lists the observed vibronic transitions, all of which are of a_g symmetry. On the basis of the spectroscopic convention, these modes are numbered 1−29 in the order of decreasing frequencies. The resulting scaling factor based on a least-squares fitting is 0.964, with a coefficient of determination (R^2) of 0.9998.

dx.doi.org/10.1021/jp303323e | J. Phys. Chem. A 2012, 116, 7016−7022

Table 1. Observed and Calculated Vibrational Frequencies for the Excited Electronic State of Chrysene[a]

experiment	calculation[b]	assignment
278	281	$55^{1}54^{1}$
290	283	29^{1}
543	**532**	**26^{1}**
655	**666**	**25^{1}**
752	755	24^{1}
842	835	$28^{1}27^{1}$
851	**851**	**23^{1}**
1237	1245	16^{1}
1343	1346	14^{1}
1369	1369	13^{1}
1442	1441	10^{1}

[a]All observed modes are of a_g symmetry, and only the bold-faced transitions have yielded observable ZEKE spectra. [b]A scaling factor of 0.964 is included in the calculation result.

Previous spectroscopic reports on the vibronic structures of chrysene are limited.[37] The work by Borisevich et al. using laser-induced fluorescence and dispersed fluorescence techniques has identified the majority of the a_g modes of the S_1 state.[37] Our assignments of the band origin and most of the features below 1250 cm^{-1} are the same as those of Borisevich et al., but higher vibrational bands differ both in experimental values and in assignment.

ZEKE Spectroscopy. By setting the resonant laser at each vibronic transition observed in the REMPI experiment and scanning the ionization laser, we attempted to obtain ZEKE spectroscopy of the cation. However, this effort was only successful for the origin band and modes 23, 25, and 26. The intensity of mode 13 is comparable to those of the lower frequency modes in Figure 1, but repetitive efforts resulted in no ZEKE signal. In addition, the ZEKE spectra obtained via the origin and via mode 25 were about an order of magnitude stronger than those from modes 26 and 23. Figure 2 shows the resulting spectra, with qualitative indications of the signal intensity. The identity of the vibrational level of the intermediate state for each ZEKE spectrum is labeled in the corresponding panel by a black dot. The experimental and theoretical values are shown in Table 2, and the assignment of the cation is noted by a superscript "+". Limited by the line width of the resonant transitions and the pulsed electric field, the uncertainty of the experimental values of the ZEKE spectra is 7 cm^{-1}.

The spectrum from the origin band in the bottom panel is by far the most intense, resulting in the appearance of several low-frequency a_g modes of the cation that were unobservable in the REMPI spectrum. From the energy of the origin band, taking into consideration the shifts due to the pulsed ionization field in the ZEKE experiment, the ionization threshold is determined to be 61 219 cm^{-1}. This value is 163 cm^{-1} above that reported by Schmidt from photoelectron spectroscopy.[2]

Vibrational assignment of the observed bands was mostly based on our calculation of the cationic state using the density functional theory method, the B3LYP functional, and the 6-311G(d,p) basis set. The FC calculation of the ZEKE spectrum from the origin of the S_1 state is shown in Figure 3. Given the limited qualitative agreement in the REMPI spectrum of Figure 1, the agreement in Figure 3 is quite remarkable. Although the origin band is still too strong for the calculation, the distribution of vibrational modes is every similar between the

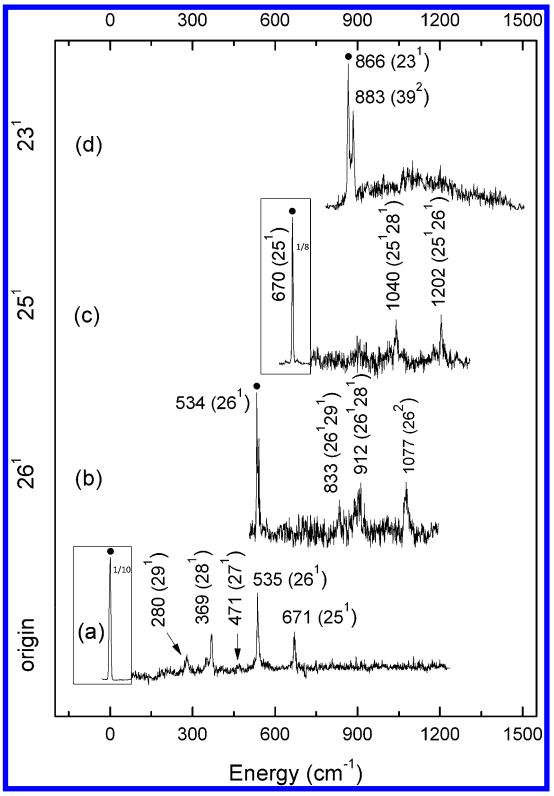

Figure 2. Two-color ZEKE spectra of chrysene recorded via different vibrational levels of the intermediate electronic state: (a) 0^0, (b) 26^1, (c) 25^1, and (d) 23^1. The energy in the *x*-axis is relative to the ionization threshold at 61 219 cm^{-1}. The assignment in the figure refers to the vibrational levels of the cation, and the corresponding vibrational level of the intermediate state is labeled by a black dot in each panel.

Table 2. Observed and Calculated Vibrational Frequencies of Chrysene Cation

intermediate vibronic level				cation	
origin	26^1	25^1	23^1	calculation[a]	assignment[b]
0				0	origin
280				280	29^+
369				368	28^+
471				466	27^+
535	534			545	26^+
671		670		671	25^+
	833			826	26^+29^+
			866	864	23^+
			883	890	39^{2+} (b_g)
	912			913	26^+28^+
		1040		1040	25^+28^+
	1077			1090	26^{2+}
		1202		1216	25^+26^+

[a]A scaling factor of 0.9766 is included in the calculation result. [b]All modes are of a_g symmetry except for mode 39^+ (b_g), as noted.

two spectra. On the basis of the spectral assignment, a least-squares fitting of the observed fundamental frequencies of modes 23–29 resulted in a scaling factor of 0.9766 with a R^2 value of 0.9994. The reduction in theoretical vibrational frequencies reduces the deviation from experimental values to within 6 cm^{-1}, except for mode 26, in which case the theoretical value is 9 cm^{-1} above that of the experiment. This scaling factor

dx.doi.org/10.1021/jp303323e | J. Phys. Chem. A 2012, 116, 7016–7022

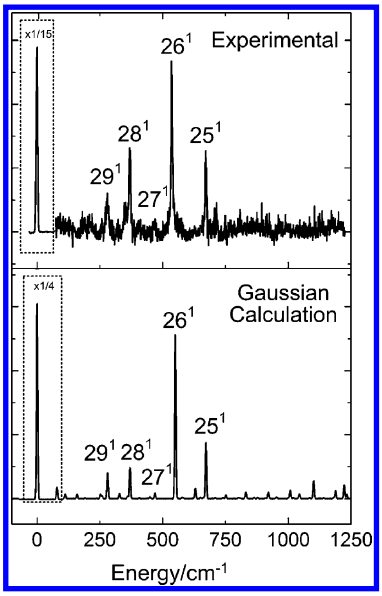

Figure 3. Comparison between experimental (top) and simulated (bottom) ZEKE spectra from the origin of the S_1 state.

is within the range of those of Langhoff[41] but smaller than our previous values from other PAHs.[8,33,34] In particular, our earlier studies of tetracene and pentacene have both concluded the high accuracy in frequency calculations from DFT for the cation,[33,34] and no scaling was needed to fit the experimental values.

Regardless of the overall strength of the ZEKE signal, interestingly, all spectra are dominated by the same vibrational mode of the intermediate state, and all the combination bands of each individual spectrum contain the same vibrational mode as that of the intermediate state, except for trace d. This observation is in line with the propensity rule observed from our previous studies of PAHs[8,33,34] and a series of substituted benzene derivatives.[42−44]

The weaker ZEKE spectra from modes 26 and 23 both demonstrate a doublet feature for the strongest band, and assignment of these bands has proven challenging. In the top panel d, the separation of the doublet is nearly 20 cm^{-1}, but no other fundamental modes of a_g symmetry from calculation are close to the value of 883 cm^{-1} after scaling. However, the fundamental frequency of a b_g mode and a second harmonic of yet another b_g mode are both close in energy to the observed band. Taking the symmetry selection rule into consideration, we therefore tentatively assign the higher energy component $39b_g^{2+}$. The doublet feature in panel b from mode 26 has a splitting of 7 cm^{-1}, and in Table 2, mode 26 demonstrates the largest deviation between calculation and experiment. At ∼540 cm^{-1}, this band is unlikely to be the second harmonic of lower frequency Franck−Condon forbidden modes with non-a_g symmetry, since our calculation only shows six modes that are below the fundamental frequencies of $29a_g$ at 280 cm^{-1}, none of which is even close to the transition frequency within 100 cm^{-1}. Currently, we do not have an explanation for this doublet splitting.

Our ZEKE result complements previous work on infrared spectroscopy of PAH cations using matrix isolation spectroscopy.[40] In the work of Hudgins and Allamandola,[40] IR active modes from 676 to 1593 cm^{-1} were reported. Even within the overlapping spectral region, none of our modes are IR active;

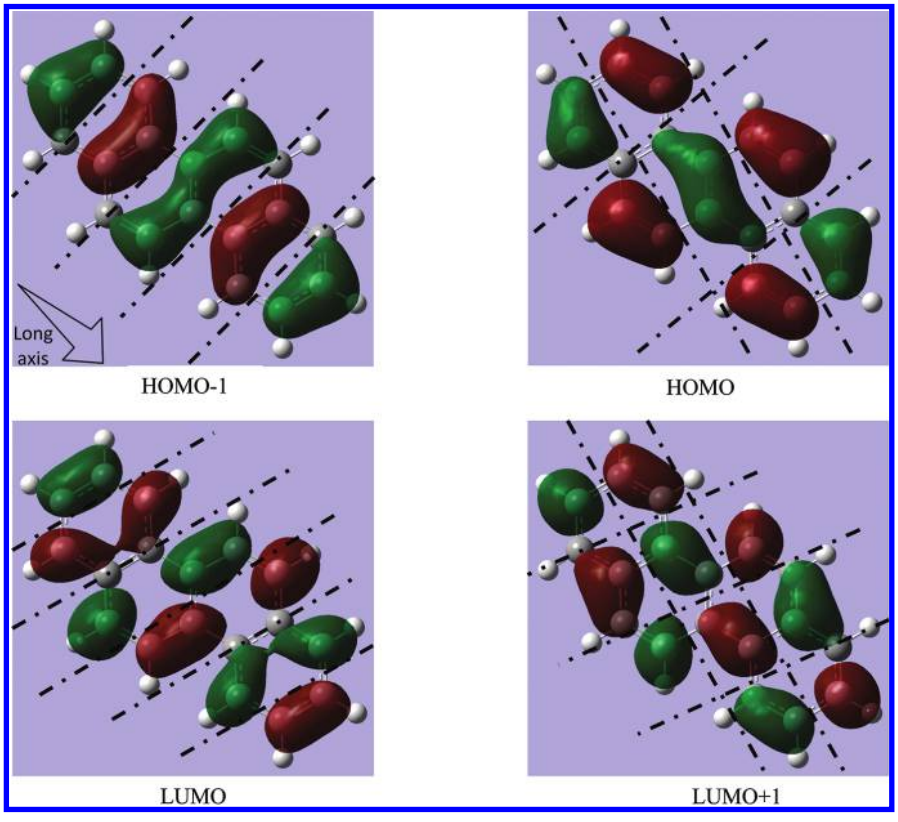

Figure 4. Calculated molecular orbitals of chrysene with nodal planes. The broad arrow in the top panel for the HOMO represents the general direction of the long axis in the discussion.

dx.doi.org/10.1021/jp303323e | J. Phys. Chem. A 2012, 116, 7016−7022

hence, our results offer more data points for the vibrational spectroscopy of the cation. Combination of the two different types of measurements offers the possibility of global fitting for the best scaling factor, which could assist with astrophysical modeling and chemical identification of PAH compounds.

DISCUSSION

Electronic State. The calculation for the vibrational frequencies of the electronically excited neutral state was obtained by setting the keyword in Gaussian 09 root = 2, i.e., we believe that the TDDFT calculation reversed the order of the S_1 and S_2 states.[8] This belief is based on our analysis of the molecular orbitals and previous theoretical and experimental reports.[2,3,36,38] Figure 4 shows the highest occupied molecular orbital (HOMO), the next lower energy orbital HOMO − 1, the lowest unoccupied molecular orbitals (LUMO), and the next higher energy orbital LUMO + 1 with the corresponding nodal planes. The HOMO and HOMO − 1 orbitals both have four nodal planes each, and the LUMO and LUMO + 1orbitals both have five nodal planes each. This qualitative result implies that the energies of the HOMO and HOMO − 1 orbitals are probably similar, while those of the LUMO and LUMO + 1 orbitals are similar. A potential complication is thus configuration interaction, which could result in a wrong order from the straightforward calculation. Our previous experience with peri-condensed PAHs has confirmed this situation,[8−10] and to obtain a reasonable vibrational assignment, the keyword has to be set with root = 2 for pyrene, B*a*P, and B*ghi*P.

The distribution of the nodal planes is also indicative of the nature of the electronic transitions and the direction of the transition dipole. Due to the low symmetry of the molecular structure, the nodal planes do not have a consistent direction, and for the ease of discussion, we designate the long axis to be along the general direction shown by the arrow in the inset of the HOMO. We notice that both near-degenerate transitions of HOMO − 1 to LUMO and HOMO to LUMO + 1 involve the addition of a nodal plane along the long axis of the molecular frame, and the transition dipoles should therefore be along the long axis. The HOMO−LUMO transition, on the other hand, involves multiple rearrangements of nodal planes: those along the long axis are increased from 2 to 5, and those along the short axis disappear. The direction of the transition dipole, however, should still be along the long axis. We therefore expect two electronic transitions that are of similar energies and of the same symmetry, one from the HOMO−LUMO transition, and the other from the nearly degenerate pair of HOMO − 1 to LUMO or HOMO to LUMO + 1. This situation of chrysene is drastically different from that of tetracene, where the nodal planes of HOMO − 1, HOMO, LUMO, and LUMO + 1 increase consecutively from 3 to 6. In this clear-cut case of tetracene, the Gaussian program, regardless of calculation method, has no problem in calculating the order and symmetry of related electronic states.

Our belief that the S_2 state from TDDFT is actually the observed electronic state agrees with previous experimental and theoretical reports.[2,3,36,38] According to Schmidt,[2] the electronic transitions in PAHs could be categorized into two cases, and chrysene belonged to case B with the lowest transition α (^1L_b) type and a transition dipole moment along the long axis. In contrast, tetracene belonged to type A with the lowest transition p (^1L_a) and a transition dipole along the short axis. Schmidt also suggested that this inversion in transition order of case B molecules was due to the strong configuration interactions of the nearly degenerate transitions of HOMO − 1 to LUMO and HOMO to LUMO + 1. This inversion would happen if the difference in orbital energies between HOMO and HOMO − 1 was less than 0.5 eV. From polarization dependence of two photon excitation spectroscopy, Liem et al. confirmed the symmetry of the first electronically excited state at ∼27 730 cm^{-1} to be ^1B_u (^1L_b).[36] From single photon excitation at 257 nm, Langelaar et al. observed dual fluorescence from chrysene corresponding to two electronically excited states separated by ∼4000 cm^{-1},[38] and the lower component was considered ^1L_b of chrysene. The fluorescence lifetime was also observed to decrease with increasing internal energy. Nijegorodov and Winkoun established a correlation diagram for the electronic energy levels of a few cata-condensed PAHs,[3] and their analysis agrees with our results on both chrysene and tetracene. The linear and magnetic circular dichroism measurements by Spanget-Larsen, Waluk, and Thulstrup[39] reported two closely spaced electronic states of chrysene, and the S_1 state at 27 600 cm^{-1} was assigned to the ^1L_b state. However, the authors concluded on a transition dipole direction along the short axis, opposite to the general belief of a ^1L_b transition.

In our previous work on pyrene, where similar confusion of S_1 and S_2 states was reported,[8] some evidence for the inversion in state order was obtained from assignment of the vibrational spectroscopy. For chrysene, this effort was futile partially because of the small number of observed modes. Furthermore, the two electronically excited states have the same symmetry, and vibronic coupling does not activate any new types of modes. The corresponding vibrational frequencies of both electronic states are also similar, and we only need to adjust the scaling factor slightly to obtain the same assignment in terms of mode number and fitting quality for both states. In this sense, the experimental vibrational frequencies cannot offer any definitive clue as to the nature of the observed electronic state.

The unusual discrepancy between calculation and experiment for the REMPI spectrum in Figure 1 is puzzling considering the fact that even when there was an ordering problem with the excited electronic states of B*ghi*P and B*a*P,[9,10] we were able to duplicate the REMPI spectra by setting "root = 2" in our CIS calculations and by taking HT coupling into consideration. For chrysene, neither CIS nor TDDFT could improve the agreement to any observable degree, with or without HT coupling. Perhaps more extensive configuration calculations, such as complete active space self-consistent field or perturbation theory methods, are required for this system.

Transition from S_1 to D_0. The overall intensity of a ZEKE spectrum from different intermediate vibronic levels of S_1 demonstrates mode dependence: the fundamental frequency of mode 25 is in between those of modes 23 and 26, but the intensity of its ZEKE spectrum is about 1 order of magnitude stronger. In addition, the intensity of mode 13 in Figure 1 is similar to those of modes 23−26, but there was no ZEKE signal to be observed in our experiment. Although we do expect that the stabilities of ZEKE Rydberg states decrease with increasing internal energy of the ionic state, the strong ZEKE signal for mode 25 is inconsistent with this trend. The calculation in Figure 3 shows regular Franck−Condon behavior for mode 25 when ionized from the origin band of the S_1 state. However, opposite from all previous studies of ZEKE spectroscopy of PAHs,[8−10,33,34] the origin band from calculation is actually a few folds weaker than that from the experiment. In Figure 1, the calculation of the REMPI spectrum considerably under-

estimates the intensities of modes 25 and 23. These discrepancies are all manifestations of complicated vibronic dynamics in the seemingly simple molecule chrysene. To our knowledge, there has been just one similar report in the literature on vibrational mode dependence of ZEKE states.[45] In the work from Grant's group on three photon ionization of NO_2,[45] the ZEKE intensity was observed to be weaker for the symmetric stretching mode than for other modes of the cation, and vibrational autoionization of ZEKE Rydberg states was proposed for this intensity abnormally. In diatomic molecules such as CO,[46] some degree of relaxation between two nearly degenerate series of Rydberg states was proposed, but by and large, the ionic core was proven to exert minimal effect on the Rydberg electron, even when the core goes through radiative decay or dissociation.[47,48]

Nevertheless, each ZEKE spectrum in Figure 2 is dominated by one single transition, showing clear preference for preserving the vibrational excitation of the intermediate state. This propensity is considered a sign of molecular rigidity during ionization.[8,33,34,42−44] In this aspect, chrysene seems to have even more capacity to accommodate the additional charge than tetracene.[34] Similar to tetracene, Mulliken population analysis also reveals that the central rings have more positive charges than the side rings: 0.30 vs 0.20 electrons, in agreement with the reactivity of different carbon atoms from organic chemistry.

Comparisons with Tetracene and Other PAHs. In our previous work on tetracene and pentacene prior to the availability of Gaussian 09,[33,34] we have reported excellent agreement between the experimental and DFT calculations for the frequency of the cation. However, the intensity distributions were way off. The availability of TDDFT and Herzberg−Teller coupling and our success with a few peri-condensed PAHs[8−10] prompted us to revisit the calculation of the two cata-condensed PAHs. Unlike the cases of peri-condensed PAHs and chrysene, neither tetracene nor pentacene is plagued by two nearby electronic states; hence, there is no confusion as to the molecular orbitals of the excited state, and vibronic coupling should be minimal. Figure 5 shows the REMPI and ZEKE spectra of tetracene overlapped with our new calculation using the Gaussian 09 suite. Both the neutral and ionic ground state were calculated using DFT with the B3LYP functional and the 6-31G basis set, and the electronic excited state was obtained using TDDFT with the 6-31G basis set. The calculated REMPI spectrum in Figure 5 was obtained with the HT option, but the results remain the same even without vibronic coupling. For pentacene, however, the situation is still hopeless for any qualitative agreement in the intensity distribution, with or without the HT option.

The additional kink in the molecular structure of chrysene seems to have an effect not only on the molecular orbitals and the relaxation dynamics of vibronic states, but also on the rigidity of the molecular frame of the cation. In the case of tetracene, one out-of-plane mode was observed in both the REMPI and the ZEKE spectra, while in chrysene, only in the ZEKE spectrum is one out-of-plane mode observable. The lower symmetry of chrysene seems to have enhanced the rigidity of the cation, in agreement with our previous conclusions on a few peri-condensed species.[8−10] For pentacene, in contrast, only out-of-plane rippling modes of the ribbon were observed, and no FC allowed transitions were detected. Pentacene is perhaps an extreme case that cannot be resolved with our limited computational resources.

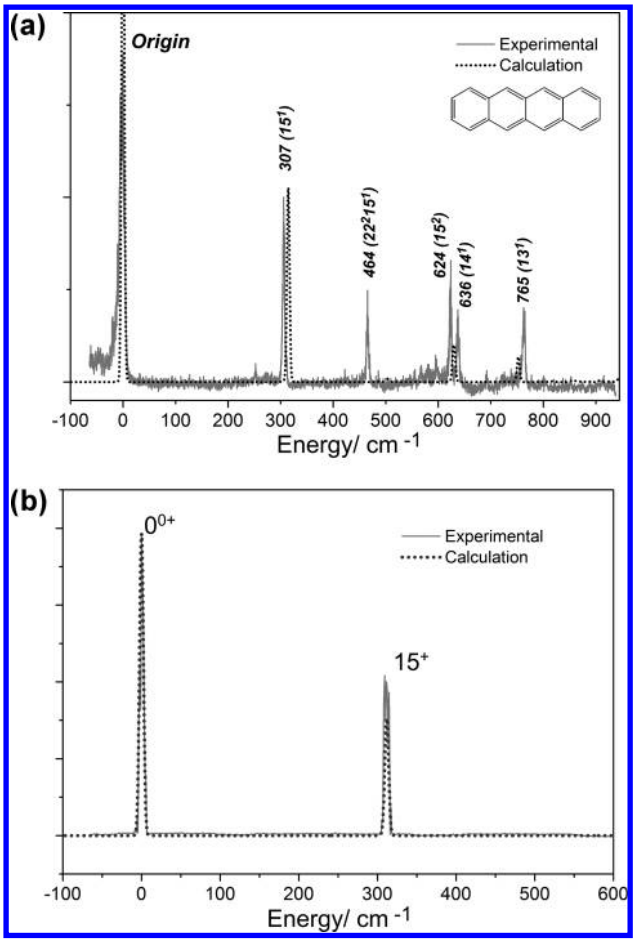

Figure 5. REMPI (a) and ZEKE (b) spectra of tetracene from the origin band of the REMPI spectrum. The gray lines are calculations using DFT (a) and TDDFT (b) from Gaussian 09, and the dotted lines are experimental results from ref 34. The frequency scaling factor for the REMPI spectrum is 0.9862, but no scaling is necessary for the ZEKE spectrum from the origin band of S_1.

Among the sampled PAHs that demonstrate reasonable agreements between calculations and experiments, tetracene[34] is an isomer of chrysene, and the peri-condensed systems[8−10] span a range of sizes, with some being smaller while others bigger than chrysene. The success of these samples makes it difficult to understand the discrepancy in the REMPI spectrum of chrysene in Figure 1. In addition, the frequency calculations for cata-condensed PAHs tetracene and pentacene require no scaling,[33,34] but the situation is different for chrysene.

CONCLUSION

Compared with tetracene, chrysene is only different by a kink in the fused hexagonal chain. Yet this kink seems to wrack havoc, both in terms of molecular orbitals and vibrational frequencies. Configuration interaction dominates the first electronic transition, and careful tweaking of the calculation keywords is needed to obtain the correct nature of the relevant electronic state. The stability of the ZEKE Rydberg states, on the other hand, demonstrates a dependence on the vibrational mode of the ionic core. Although for the straight cata-condensed polyacenes such as tetracene and pentacene, DFT calculations have proven reliable in predicting the vibrational frequencies of the cations, a kink in the linear structure calls for a scaling factor of 0.9766 from the calculation. Our conclusion

dx.doi.org/10.1021/jp303323e | J. Phys. Chem. A 2012, 116, 7016−7022

demonstrates the complexity of this seemingly simple group of PAH compounds.

AUTHOR INFORMATION

Corresponding Author

*E-mail: wei.kong@oregonstate.edu. Fax: 541-737-2062. Phone: 541-737-6714.

Notes

The authors declare no competing financial interest.

ACKNOWLEDGMENTS

This work is supported by the National Aeronautics and Space Administration under award No. NNX09AC03G.

REFERENCES

(1) Becker, R. S.; Singh, I. S.; Jackson, E. A. *J. Chem. Phys.* **1963**, *38*, 2144.
(2) Schmidt, W. *J. Chem. Phys.* **1977**, *66*, 828.
(3) Nijegorodov, N.; Winkoun, D. P. *Spectrochim. Acta, Part A* **1997**, *53A*, 2013.
(4) Tanaka, J. *Bull. Chem. Soc. Jpn.* **1965**, *38*, 86.
(5) Callis, P. R. *Annu. Rev. Phys. Chem.* **1997**, *48*, 271.
(6) Bito, Y.; Shida, N.; Toru, T. *Chem. Phys. Lett.* **2000**, *328*, 310.
(7) Dierksen, M.; Grimme, S. *J. Chem. Phys.* **2004**, *120*, 3544.
(8) Zhang, J.; Han, F.; Kong, W. *J. Phys. Chem. A* **2010**, *114*, 11117.
(9) Zhang, J.; Harthcock, C.; Han, F.; Kong, W. *J. Chem. Phys.* **2011**, *135*, 244306.
(10) Zhang, J.; Harthcock, C.; Kong, W. *J. Phys. Chem. A* **2012**, *116*, 1551.
(11) Chang, C.-H.; Lopez, G.; Sears, T. J.; Johnson, P. M. *J. Phys. Chem. A* **2010**, *114*, 8262.
(12) McRae, C.; Sun, C.-G.; Snape, C. E.; Fallick, A. E. *Am. Lab. (Shelton, CT, U. S.)* **1999**, *31*, 1.
(13) Wiersum, U. E.; Jenneskens, L. W. In *Gas-Phase Reactions in Organic Synthesis*; Vallee, Y., Ed.; Gordon & Breach: Amsterdam, 1997,; p 143.
(14) Harvey, R. G. *Polycyclic Aromatic Hydrocarbons: Chemistry and Carcinogenicity*; Cambridge University Press: London, 1991.
(15) Sami, S.; Faisal, M.; Huggett, R. J. *Mar. Biol. (Berlin)* **1992**, *113*, 247.
(16) Kriek, E.; Rojas, M.; Alexandrov, K.; Bartsch, H. *Mutat. Res., Fundam. Mol. Mech. Mutagen.* **1998**, *400*, 215.
(17) Smith, L. E.; Denissenko, M. F.; Bennett, W. P.; Li, H.; Amin, S.; Tang, M.-S.; Pfeifer, G. P. *J. Natl. Cancer Inst.* **2000**, *92*, 803.
(18) Seufert, J.; Rambach, M.; Bacher, G.; Forchel, A.; Passow, T.; Hommel, D. *Appl. Phys. Lett.* **2003**, *82*, 3946.
(19) Knipp, D.; Street, R. A.; Volkel, A.; Ho, J. *J. Appl. Phys.* **2003**, *93*, 347.
(20) Tyutyulkov, N.; Ivanov, N.; Muellen, K.; Staykov, A.; Dietz, F. *J. Phys. Chem. B* **2004**, *108*, 4275.
(21) Allamandola, L. J.; Tielens, A. G. G. M.; Barker, J. R. *NATO ASI Ser., Ser. C* **1987**, *210*, 305.
(22) Leger, A.; d'Hendecourt, L.; Joblin, C. *Adv. Space Res.* **1993**, *13*, 473.
(23) Snow, T. P. *Spectrochim. Acta, Part A* **2001**, *57A*, 615.
(24) Bernstein, M. P.; Dworkin, J. P.; Sandford, S. A.; Cooper, G. W.; Allamandola, L. J. *Nature (London, U. K.)* **2002**, *416*, 401.
(25) Malloci, G.; Mulas, G.; Benvenuti, P. *Astron. Astrophys.* **2003**, *410*, 623.
(26) Duley, W. W. *Faraday Discuss.* **2006**, *133*, 415.
(27) Rhee, Y. M.; Lee, T. J.; Gudipati, M. S.; Allamandola, L. J.; Head-Gordon, M. *Proc. Natl. Acad. Sci. U. S. A.* **2007**, *104*, 5274.
(28) Li, A. In *Deep Impact As a World Observatory Event: Synergies in Space, Time, and Wavelength*; Kaufl, H. U.; Moorwood, A. F. M., Ed.; Springer: Berlin, 2009; p 161.
(29) Salama, F.; Galazutdinov, G. A.; Krelowski, J.; Biennier, L.; Beletsky, Y.; Song, I.-O. *Astrophys. J.* **2011**, *728*, 154.
(30) Zhang, K.; Guo, B.; Colarusso, P.; Bernath, P. F. *Science (Washington, D. C.)* **1996**, *274*, 582.
(31) Pirali, O.; Van-Oanh, N.-T.; Parneix, P.; Vervloet, M.; Brechignac, P. *Phys. Chem. Chem. Phys.* **2006**, *8*, 3707.
(32) Hu, A.; Duley, W. W. *Astrophys. J.* **2007**, *660*, L137.
(33) Zhang, J.; Han, F.; Pei, L.; Kong, W.; Li, A. *Astrophys. J.* **2010**, *715*, 485.
(34) Zhang, J.; Pei, L.; Kong, W. *J. Chem. Phys.* **2008**, *128*, 104301.
(35) Frisch, M. J. T., G. W.; Schlegel, H. B.; Scuseria, G. E.; Robb, M. A.; Cheeseman, J. R.; Scalmani, G.; Barone, V.; Mennucci, B.; Petersson, G. A.; Nakatsuji, H.; Caricato, M.; Li, X.; Hratchian, H. P.; Izmaylov, A. F.; Bloino, J.; Zheng, G.; Sonnenberg, J. L.; Hada, M.; Ehara, M.; Toyota, K.; Fukuda, R.; Hasegawa, J.; Ishida, M.; Nakajima, T.; Honda, Y.; Kitao, O.; Nakai, H.; Vreven, T.; Montgomery, Jr., J. A.; Peralta, J. E.; Ogliaro, F.; Bearpark, M.; Heyd, J. J.; Brothers, E.; Kudin, K. N.; Staroverov, V. N.; Kobayashi, R.; Normand, J.; Raghavachari, K.; Rendell, A.; Burant, J. C.; Iyengar, S. S.; Tomasi, J.; Cossi, M.; Rega, N.; Millam, N. J.; Klene, M.; Knox, J. E.; Cross, J. B.; Bakken, V.; Adamo, C.; Jaramillo, J.; Gomperts, R.; Stratmann, R. E.; Yazyev, O.; Austin, A. J.; Cammi, R.; Pomelli, C.; Ochterski, J. W.; Martin, R. L.; Morokuma, K.; Zakrzewski, V. G.; Voth, G. A.; Salvador, P.; Dannenberg, J. J.; Dapprich, S.; Daniels, A. D.; Farkas, Ö.; Foresman, J. B.; Ortiz, J. V.; Cioslowski, J.; Fox, D. J. *Gaussian 09, Revision A.1*; Gaussian, Inc.: Wallingford, CT, 2009.
(36) Liem, N. Q.; Salvi, P. R.; Marconi, G.; Orlic, N. *Chem. Phys. Lett.* **1989**, *164*, 313.
(37) Borisevich, N. A.; Dyachenko, G. G.; Petukhov, V. A.; Semenov, M. A. *Opt. Spectrosc.* **2008**, *105*, 859.
(38) Langelaar, J.; Leeuw, M. W.; Van, V. J. D. W.; Rettschnick, R. P. H. *Chem. Phys. Lett.* **1979**, *62*, 14.
(39) Spanget-Larsen, J.; Waluk, J.; Thulstrup, E. W. *J. Phys. Chem.* **1990**, *94*, 1800.
(40) Hudgins, D. M.; Allamandola, L. J. *J. Phys. Chem. A* **1997**, *101*, 3472.
(41) Langhoff, S. R. *J. Phys. Chem.* **1996**, *100*, 2819.
(42) He, Y.; Wu, C.; Kong, W.; Schultz, K. P.; Nelsen, S. F. *J. Phys. Chem. A* **2005**, *109*, 959.
(43) He, Y.; Kong, W. *J. Chem. Phys.* **2005**, *122*, 244302.
(44) Wu, C.; He, Y.; Kong, W. *Chem. Phys. Lett.* **2004**, *398*, 351.
(45) Bryant, G. P.; Jiang, Y.; Martin, M.; Grant, E. R. *J. Chem. Phys.* **1994**, *101*, 7199.
(46) Kong, W.; Hepburn, J. W. *J. Phys. Chem.* **1995**, *99*, 1637.
(47) Kong, W.; Rodgers, D.; Hepburn, J. W. *Chem. Phys. Lett.* **1994**, *221*, 301.
(48) Martin, J. D. D.; Hepburn, J. W. *J. Chem. Phys.* **1998**, *109*, 8139.